

# Application of HTS SQUIDs in Nondestructive Evaluation of Aircraft Parts and Concrete Bridges

Hans-Joachim Krause

Forschungszentrum Jülich, D-52425 Jülich, Germany

## Abstract

The challenge for applications of HTS SQUID in non-destructive evaluation is the development of mobile SQUID systems operating in hostile environments. For eddy current detection of deep-lying flaws in aircraft wheels, an automated aircraft wheel inspection system using a HTS SQUID magnetometer in conjunction with Joule-Thomson machine cooling was developed. The aircraft wheel testing is being performed with the wheel slowly rotating and a robot with the SQUID enclosure scanning stepwise along the wheel axis. A small crack with an inside penetration of only 10% of the wall thickness was found by scanning the outside of the wheel. The results of a wheel measurement campaign at the Lufthansa base at Frankfurt airport are presented.

Using SQUID eddy current testing, the detection of cracks at rivet joints and identifying corrosion damage hidden deeply in the tested structure has been shown. However, the requirement to take maps of the magnetic field, usually by meander-shaped scans, leads to unacceptably long measurement times. A solution is the development of SQUID arrays for eddy current fuselage testing. The multiplexed operation of three planar HTS rf SQUID gradiometers with one readout electronics and one cable is shown, demonstrating the advantage of lower liquid nitrogen boil-off.

For detection of tendon ruptures in prestressed members of bridges, a multi-channel SQUID system was developed. The tendons are magnetized by scanning a yoke magnet along the concrete surface. Four HTS dc-SQUID magnetometers with ramp-type junctions optimized for high-field performance are used to record the magnetic stray field. Signals from stirrups of the mild steel reinforcement are suppressed by means of a sophisticated signal analysis. Subsequent correlation analysis with the dipolar signal of a typical void yields rupture signal amplitudes. Results of measurements on a German highway bridge are presented. Rupture indications were verified as originating from broken strands by opening the bridge deck.

## 1. Introduction

Superconducting Quantum Interference Devices (SQUIDs) are the magnetic field sensors with the best field sensitivity and the largest dynamic range known to date. Following the development of SQUID sensors, many research groups worldwide have shown the use of SQUIDs in conjunction with electromagnetic Non-destructive Evaluation (NDE), see for example the review of Jenks *et al.* [1]. In this paper, we'll present two examples of prototype development conducted in the framework of joint German R&D projects with industry.

The first potential application field for SQUID NDE is aircraft testing. Aircraft, being exposed to strong forces, moisture and changing temperatures, have to be checked regularly for cracks and corrosion in order to assure for flight safety. Eddy-current testing by inductive sensors is a common NDT method in aircraft maintenance. Compared to induction coils, SQUID systems offer a higher sensitivity at low excitation frequencies, permitting the detection of deeper flaws, and an excellent linearity, allowing quantitative evaluation of magnetic field maps from the investigated structure [2,3]. The potential of eddy current testing with HTS SQUIDs has previously been demonstrated for up to 5 cm deep-lying

defects in stacks of aluminum sheets using a stationary rf SQUID gradiometer [4]. Using a sample from aircraft aluminum alloy, with a saw cut hidden deep in the material, it was shown that a HTS SQUID magnetometer system yields an improvement in signal-to-noise ratio by more than two orders of magnitude, compared to a conventional eddy current system [5]. For practical applications, the SQUID systems have to be made mobile and capable to operate without any magnetic shielding in maintenance hangars where the level of electromagnetic disturbances is very high [6,7]. In a joint R&D project, Rohmann GmbH, DASA, Lufthansa Technik AG, ILK Dresden, University of Giessen (Institute for Applied Physics) and Research Centre Jülich are trying to introduce HTS SQUIDs into aircraft maintenance. Project goal is the development of prototype SQUID systems that demonstrate of the advantages of the new technique for aircraft wheel testing or fuselage testing.

The second application field is the inspection of concrete bridges containing prestressed steel [8]. The Federal road network of Germany contains about 13,000 prestressed concrete bridges. Due to constantly growing volumes of traffic and higher loads per axle, these structures are subject to increasing loads. Regular inspections of all engineering structures consist mainly of a visual inspection, thus deterioration and damages are typically identified rather late. Non-destructive test methods (NDT) may provide a relatively quick and inexpensive means to establish whether a bridge is still in a serviceable condition. Particularly important is the non-destructive identification of the position of defects in prestressed concrete bridges, as the stability of the entire structure may be affected.

## **2. Testing of Aircraft parts with Eddy current and SQUID**

### ***2.1. The Eddy current technique***

Nonmagnetic metallic materials are usually tested by an ac technique. Using alternating currents has two significant advantages: first, the coupling of excitation to the material under test can be done inductively, thus eliminating the need for impractical electrical contacts. Second, a narrowband lock-in readout scheme can be used, resulting in noise suppression. In addition, the quadrature component containing information on excitation energy dissipation can be evaluated. Eddy current testing using a SQUID sensor is of special value in a highly safety-relevant area such as aircraft testing, where small deep flaws need to be localized and sized in aluminum structures [9]. The first demonstration of aircraft lap joint testing was performed in shielding using a LTS SQUID system [10]. Subsequently, a cryocooled LTS system with remote differential sensing coils was used to demonstrate the detection of very small, hidden flaws without shielding [11]. With the advent of HTS SQUID gradiometers for unshielded operation, appropriate excitation-detection schemes were developed [4].

### ***2.2. SQUID system components***

For portable SQUID operation, a planar gradiometer design is well suited. The rf double hole gradiometer [12] was designed for operation integrated into a hand-held system during movement in strong ambient fields commonly found in aircraft maintenance facilities. A gradiometer with a baseline of 3.7 mm and a gradient-to-flux coefficient of  $15 \text{ nT}/(\text{cm } \Phi_0)$ , with a surrounding shielding ring, is used. The gradient sensitivity of the gradiometer is approximately  $1 \text{ pT}/(\text{cm}\sqrt{\text{Hz}})$  at eddy current frequencies in the range from 110 Hz to 1 kHz. The rf SQUID readout electronics with a high slew rate allows fast scanning in strong gradient fields. This is of importance when scanning over ferromagnetic objects.

In order to do the testing directly at the aircraft, the SQUID has to be equipped with mobile cooling. A lightweight nitrogen cryostat [13], constructed by ILK Dresden for operation in any orientation, allows one a portable SQUID operation. The mobile head weighs less than 2 kg and has an operation time of 12 hours. A distance of only 3 mm between SQUID and

sample may be achieved. For a routine, stationary maintenance application such as aircraft wheel testing, SQUID cooling only needing electricity is advantageous. A commercial Joule-Thomson cryocooler (APD *Cryotiger*<sup>®</sup>) was adapted for liquid-nitrogen-free, low-noise SQUID cooling [14]. Flexible plastic gas lines allow one to position the cold head.

The eddy current excitation is applied by a differential coil. Printed multi-turn double-D coils with a diameter of 25 mm were mounted on the SQUID dewar and operated with excitation currents of up to 200 mA<sub>rms</sub>. Amplitude and phase of the eddy current response field are evaluated by a Stanford Research SR830 digital lock-in amplifier and recorded by a computer. This eddy current scheme ensures a minimum primary field at the location of the SQUID gradiometer. However, it leads to a quadrupolar signature of a small flaw.

### 2.3. Aircraft wheel testing

Aircraft wheels are subject to enormous stress and heat during take-off and landing. Because of the concentration of mechanical and thermal stress, hidden cracks emanate typically on the inside of the wheel, next to the keys on which brake structures are fastened. The cracks are covered by heat shields and therefore not easily accessible from the inside. Today, the wheels are eddy-current tested from the outside with a circumferential scan measurement, after taking off the tires. Deep flaws are detected with a low-frequency eddy current probe. However, the sensitivity is limited to large flaws: flaws with 40% wall penetration from the inside and of length twice the wall thickness can be identified reliably. In order to safely detect small hidden flaws, the wheel has to be disassembled and be tested manually from the inside, e.g. with ultrasonic equipment.

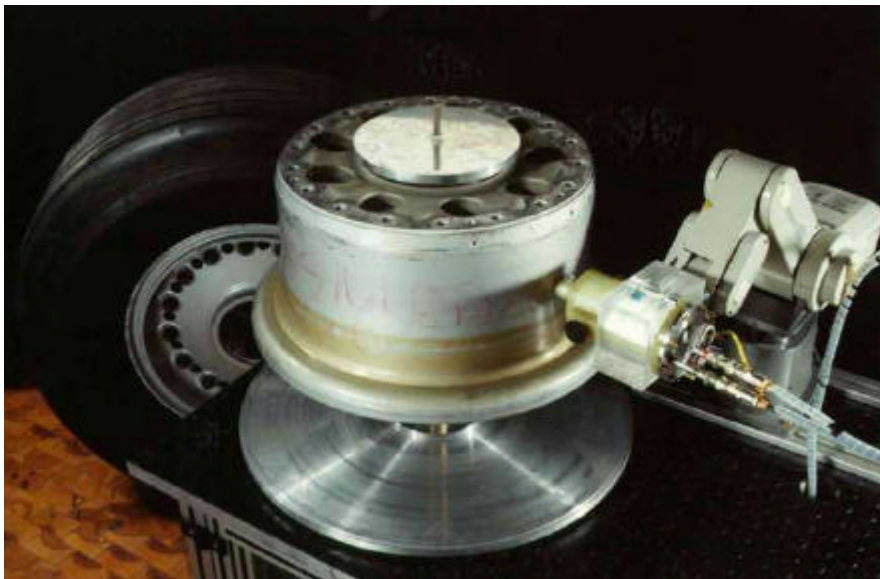


Figure 1. Setup for aircraft wheel testing with SQUID. The Joule-Thomson cold head with the SQUID mounted on top of the finger is moved along the wheel contour by a robot while the wheel is rotating.

The prototype SQUID system for wheel testing consists of an automated test stand with the wheel slowly rotating and a robot with the SQUID enclosure scanning stepwise along the wheel axis, see Figure 1. While the wheel is rotating, the robot moves the cryostat along its outer contour. Thus, a two-dimensional eddy current mapping of the outer wheel surface is performed.

During a three-day measurement campaign, the system was operated at the Lufthansa wheel testing facility at Frankfurt Airport. Figure 2 shows a sample measurement of an Airbus A300-600 wheel.

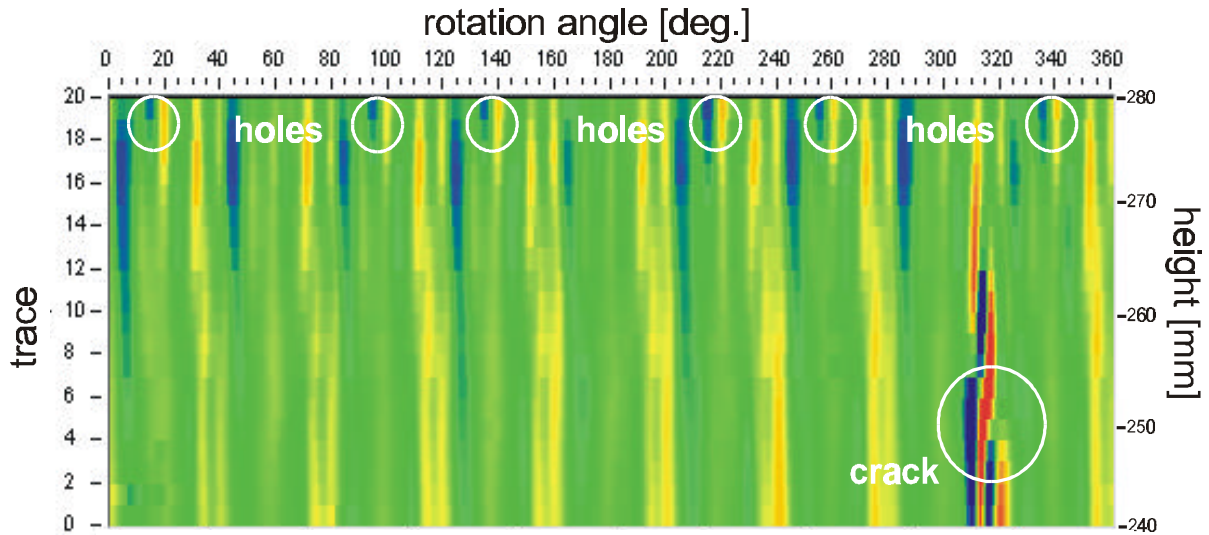


Figure 2. SQUID measurement of an Airbus A300-600 wheel (main landing gear). The measurement was conducted at Frankfurt airport, using a planar gradiometer with double D excitation (180 Hz, 130mA). The figure shows the unfiltered quadrature component of the lock-in signal. In addition to signals from 6 holes, a quadrupolar crack signature is clearly visible, located next to one of the nine keys (vertical stripes) at a height of 250 mm.

It was demonstrated that the SQUID system is capable of detecting inner flaws by automated scanning and eddy-current mapping from the outside. The smallest flaw detected with the SQUID was a 10%-flaw [15] (meaning that total wall thickness is weakened by 10% at the flaw location).

#### 2.4. Aircraft fuselage testing

Due to temperature and moisture changes in conjunction with mechanical stress, cracks and corrosion may develop in the fuselage, often located in hidden layers close to rivets. State of the art with conventional eddy current equipment is the detection of 4.5 mm long second layer cracks adjacent to rivets, underneath 2.2 mm of aluminum. For testing rivet rows, a planar HTS SQUID gradiometer was mounted in an orientation-independent cryostat, equipped with a double-D excitation coil and affixed to a fuselage surface scanner, see Figure 3.



Figure 3. Aircraft fuselage testing using a mobile SQUID system with a x-y-scanner. The flexible scanner is affixed to the fuselage with suction cups. The SQUID is scanned in a meander-like path, thus yielding an eddy-current map of the fuselage section under test.

Figure 4 shows a typical scan of a fuselage section. Using the planar gradiometer sensor and the differential excitation coil, each rivet yields a quadrupolar signal as can clearly be seen in the scan map. The rivet and the rivet hole give a strong signal even if there is no additional fault like a crack. By software windowing of the impedance trace, the flaws are identified. The flaws can be located at the rivet, see map of the evaluated signal in Figure 4. For comparison, a conventional eddy current scan is also presented.

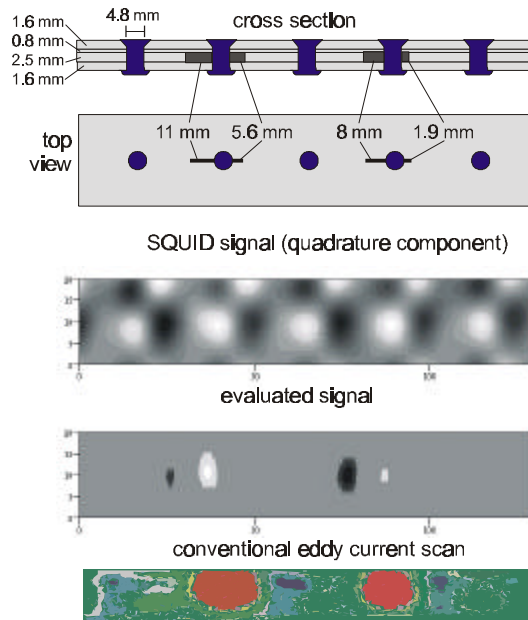


Figure 4. SQUID measurement of a calibration sample from DASA. The scan was performed with the planar SQUID gradiometer with multi-D excitation of 10 mA at 780 Hz. The scan area of 130 mm  $\times$  20 mm covers 5 rivets with 4 flaws, as sketched. They clearly show up in the evaluated scan.

However, the requirement to take maps of the magnetic field, usually by meander-shaped scans, leads to unacceptably long measurement times. Due to their inductive coupling to a tank circuit, several rf SQUID sensors may be read out sequentially by selectively coupling to their tank circuits, using only one electronics with a multiplexer [16]. A system with multiplexed operation of three planar HTS rf SQUID gradiometers, operated with one electronics and one cable, is currently under development. The multiplexed SQUID sensors were implemented in conjunction with an eddy current excitation and lock-in readout. Scanning is performed while continuously switching the operating SQUID, thus obtaining three traces simultaneously [17].

### 3. Bridge inspection using the magnetic stray field technique and SQUID

The magnetic stray field measuring method is well suited for the inspection of prestressed steel in concrete bridges [18,19,20,21]. The steel acts as a high permeability magnetic field guide. Cracks in the reinforcement bars are interruptions of that guide, thus giving rise to a leaking stray field. Typically, the flaw signal is hidden among signals of mild steel reinforcements (stirrups) located close to the concrete surface. Provided that the magnetic field sensors have sufficient sensitivity and linearity, flaw signals may be separated from structural disturbance signals by means of a specially developed signal analysis. A newly developed system incorporating four SQUID sensors for the inspection of rebars in bridges is presented [8]. The equipment has already been successfully used in field measurements.

### 3.1. Magnetic stray field technique

The principle of the magnetic stray field measurement technique is as follows: the tendon hidden in the concrete is magnetized using an exciting magnetic field  $H_0$  applied from the outside of the concrete by means of a yoke magnet. This exciting field generates a magnetization in the reinforcement bars. Local disturbances of the distribution of this magnetization due to ruptures or reductions of the cross section cause the emanation of a magnetic leakage flux (stray field) from the member. For the generation and the measurement of the stray field, a probe containing the magnetization device (yoke magnet) and the sensors is moved along the direction of the prestressed tendon outside the concrete surface (see Figure 5).

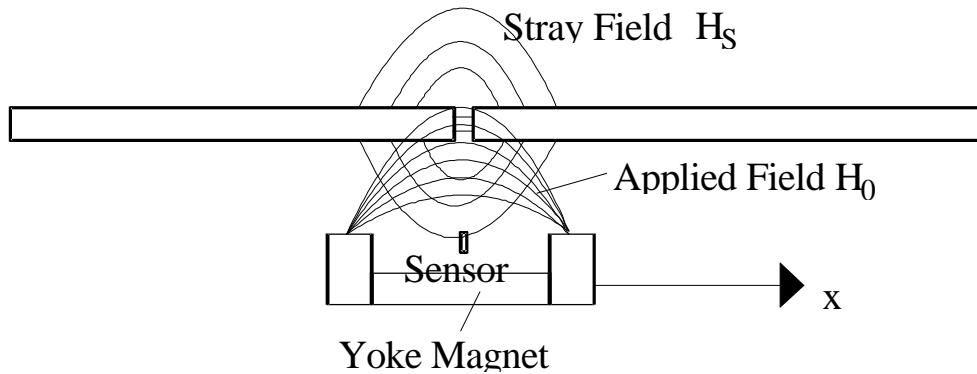


Figure 5. The principle of magnetic leakage flux measurement.

The stray field measurement is either conducted during magnetization by the exciting field (active field) or as a residual field measurement. In the latter case, the stray field is caused by the remanent magnetization of the steel after switching off the magnetization device. In the active field measurement, ruptures of the longitudinal rebars appear as a local maximum. It has been shown that a single cracked rebar can be found in post-tensioned members, even though the magnetic signature of the crack is damped significantly due to the shielding effect of the surrounding flawless rebars and the jacket tube around the bars.

### 3.2. Signal analysis

The stray field signals are affected not only by ruptures of the tendon under consideration but also by the stirrups close to the probe. Signal analysis methods for the suppression of signals from the stirrups were developed [20,8]. The magnetic signature of a stirrup shows a considerably different shape in the active field, in comparison to the residual measurement. Due to the hysteresis behavior of the ferromagnetic material, the active field signal of a stirrup has an asymmetrical shape. The polarity of the antisymmetrical residual field measurement signal of the stirrup depends on the location where the yoke magnet has been switched off during the preceding magnetization of the member. A typical stray field and two residual field signals of a single stirrup are shown in Figure 6. The residual field measurement R1 is performed after the yoke magnet is switched off at the end of the measurement length. In contrast, the measurement R2 denotes the case where the exciting field is switched off at the starting position after a full magnetization scan. The residual field signature R2 of the stirrup is inverted compared to R1.

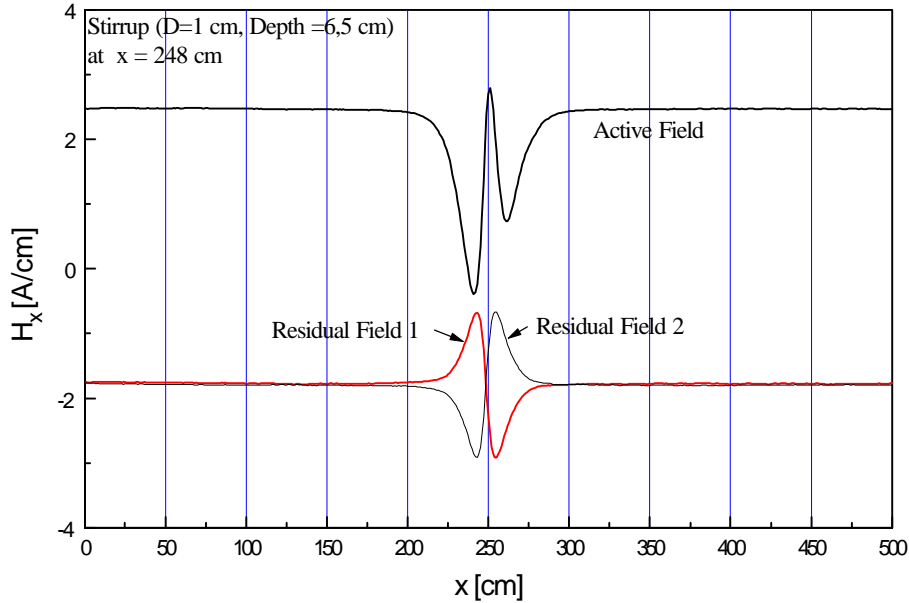


Figure 6. Stray field and remanent field signals of a stirrup [20]. The remanent field R1 was measured after switching off the yoke magnet at  $x = 500$  cm, the residual field R2 was recorded after turning off the magnet at  $x = 0$ .

This feature directly leads to the first method of stirrup signal suppression: Addition of the two residual field measurements R1 and R2 suppresses the residual field signals of the stirrups, whereas rupture signals are unaffected. Figure 7 (left) shows an example for this approach. Nevertheless, the polarity of the residual field signature of a rupture is not well defined. It depends on the magnitude of the preceding magnetization, the cross section of the flaw, and the distance probe-tendon. Due to this non-uniformity, the exclusive use of the residual field measurement for the evaluation of the integrity of tendons seems not to be sufficient [18]. The position of the stirrups can be obtained from the local maxima (R2) or minima (R1) of the derivative of the axial residual field component.

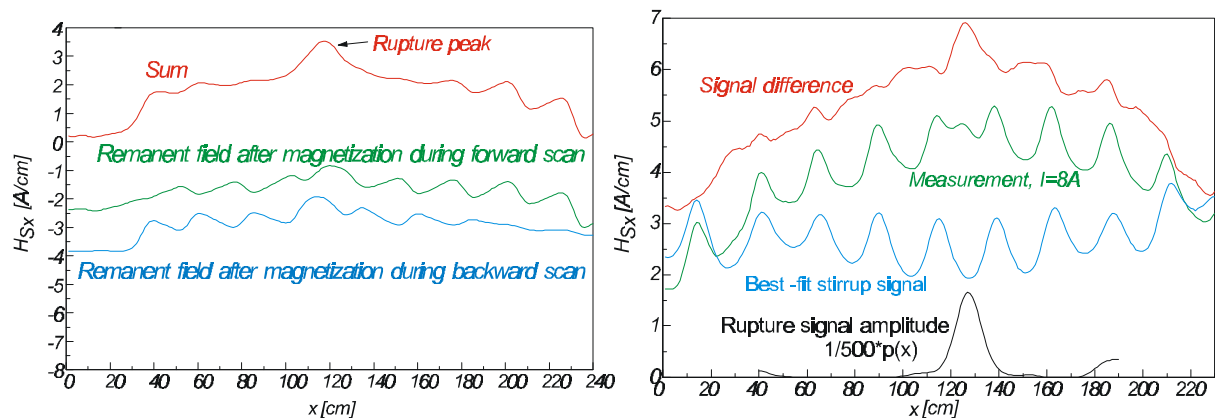


Figure 7. Examples of the elimination of stirrup signals. Left: adding two remanent field measurements with inverse magnetization polarity of the stirrups, right: Best-fit correction of stray field measurement.

In order to separate the signals from the reinforcement close to the surface, several active field measurements are conducted at successively increasing magnitude of the exciting field. Because of the strong decrease of the exciting field with distance, the measurement at low excitation fields gives dominating signals from the mild steel reinforcement close to the surface. Due to magnetic saturation, increasing excitation field only slightly alters the



magnetization of the steel close to the surface. The signal increase at higher values of the exciting field  $H_0$  is mainly caused by the steel structures (rebars) deeper in the concrete.

The second technique for the elimination of the signals from the stirrups is direct subtraction of idealized signals. First, the exact position of the stirrups is calculated from a residual field signal. Then, the signal portion of the stirrups is determined by means of the best fit method with regard to the signal of a single stirrup (Figure 6). Finally, the signal portion of the stirrups is subtracted from the measured signal. The essential portion of the signals of the tendon remains (Figure 7, right).

### 3.3. SQUID magnetometer sensors

For this application, HTS dc SQUIDs which can be operated in strong magnetic fields were developed [22], see Figure 8. The SQUIDs contain two YBCO/PBCO ramp-type Josephson junctions and a washer with slits. The field-to-flux coefficient was measured to be  $600 \text{ nT}/\Phi_0$ . When exposed to our maximum excitation fields (up to 15 mT), no degradation of performance was found. The observed increase in low frequency noise (Figure 1, right) is due to  $1/f$  noise of the current source driving the excitation magnet. For cooling the SQUID sensor array, a mobile liquid nitrogen cryostat was developed. Since the SQUID is mounted on a sapphire finger in the vacuum space of the cryostat, it can be operated orientation-independent. One refill of liquid nitrogen lasts for a working day.

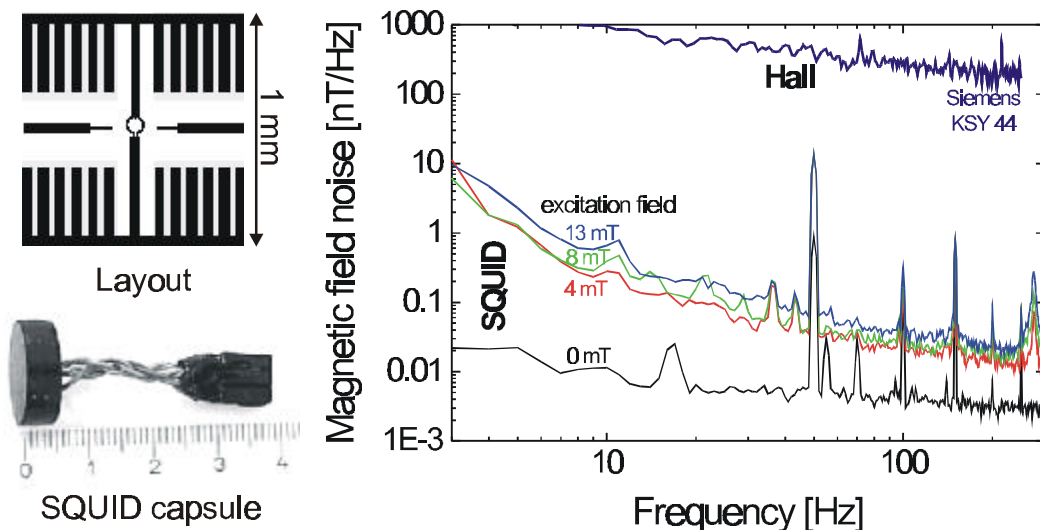


Figure 8. Packaging, Layout and magnetic field resolution of the SQUID sensors used for rebar inspection.

### 3.4. Setup of the bridge inspection system

The system consists of 4 SQUID magnetometers. They are mounted on sapphire fingers oriented radially in the liquid nitrogen cryostat. Thus, the SQUIDs measure the longitudinal field component, in scanning direction. The cryostat is fixed in a yoke magnet on the translation stage. In order to check consistency with the previous measurement technique, 4 Hall probes are also integrated with the system. A multi-channel readout and control electronics, using digital signal processors for the SQUID flux-locked loop and signal preprocessing [23], is used to acquire the data from the magnetic sensors and the position encoder. Due to the implemented flux quanta counting, the digital SQUID electronics achieves a dynamic range of  $195 \text{ dB}/\sqrt{\text{Hz}}$  with the high-field magnetometers. It is connected to a computer via an optical link. Figure 9 shows schematically the setup of the system.



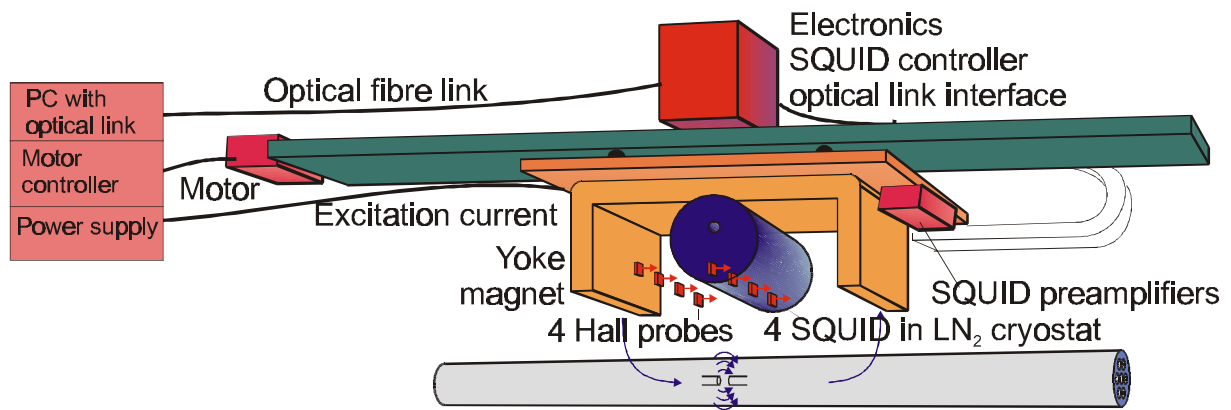


Figure 9. Schematic setup sketch of the SQUID system for magnetic inspection of rebars.

### 3.5. Measurements on a German highway bridge

As an example for a field test of the system, we present results of SQUID measurement on the valley bridge Michelsrombach (A7 near Fulda) [24,25]. At selected measurement positions, tendons were localized using the Ground Penetrating Radar (GPR) SPR-Scan from ERA Technology with a 1 GHz antenna. Subsequently, magnetic measurement scans were performed along the marked tendons, see Figure 10.

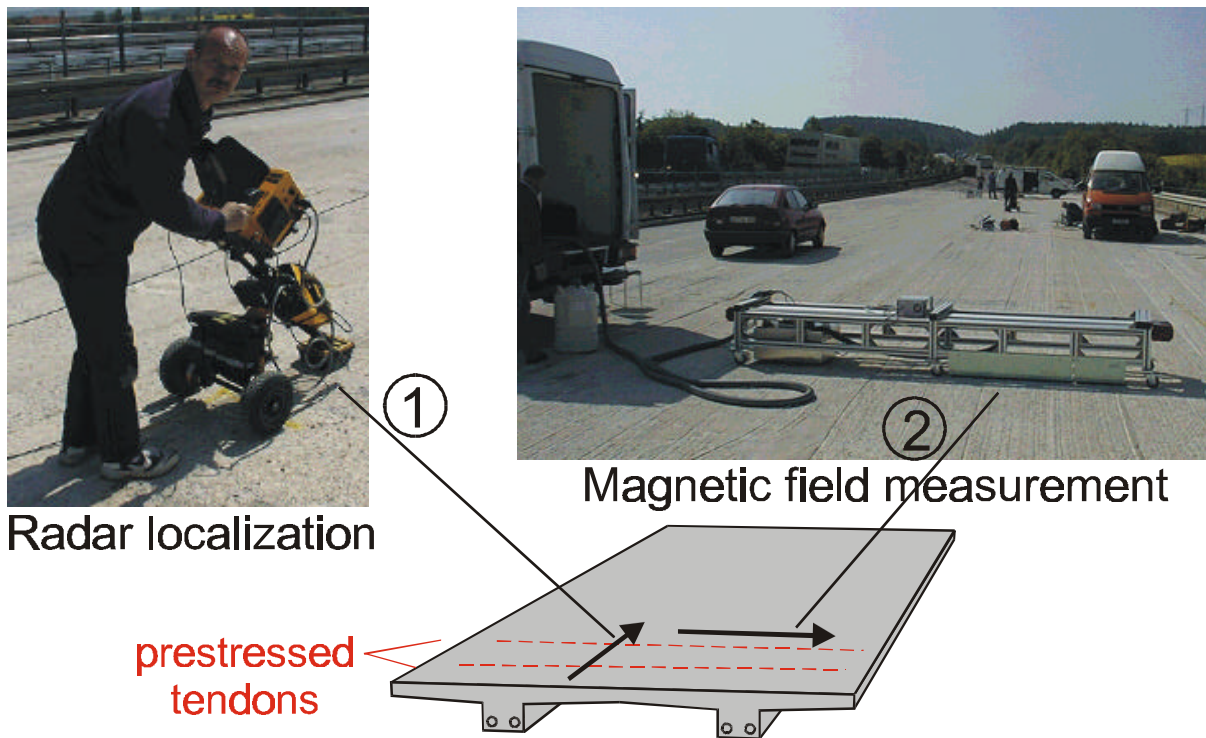


Figure 10. Schematic of the measurements conducted on the valley bridge Michelsrombach. First, the tendons were localized using Ground Penetrating Radar (①). Subsequently, the prestressed steel rebars were inspected by scanning the yoke with the SQUID system along the member (②).

After Radar localization, magnetic measurement scans were performed along the tendons. The investigation was carried out in scan segments of 260 cm length. At every location, nine scans were conducted. After a recording of the pre-existing field, scans with increasing exciting field were performed, followed by scans with decreasing field and subsequent remanent field scans after different premagnetization states. Before each measurement scan, the SQUID sensors were heated just above the critical temperature of the superconducting film in order to

eliminate trapped magnetic flux. The scan velocity was 0.1 m/s. Due to the SQUID heating, the total measurement time at one location was 20 min.

Figure 11 shows the correlation coefficient and the crack signal amplitude of the evaluated stray field and remanent field scans at a selected location of the bridge.

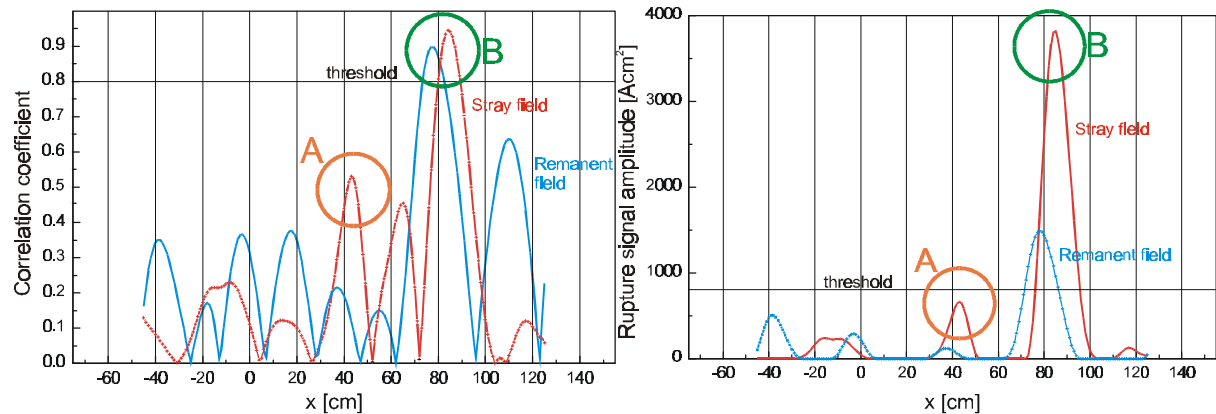


Figure 11. Correlation coefficients and Rupture signal amplitudes.

Indication A at  $x = 45$  cm yielded a correlation coefficient and a rupture signal amplitude below threshold. Opening of the concrete and the jacket tube protecting the rebars showed that the indication emanated from a loose end of a rebar, see Figure 12 A. Indication B at  $x = 82 \pm 5$  cm, however, gave an correlation coefficient and a rupture signal amplitude well above our threshold. The opening of the bridge deck (Figure 12 B) confirmed that two of the eight rebar wires were cracked at this location.

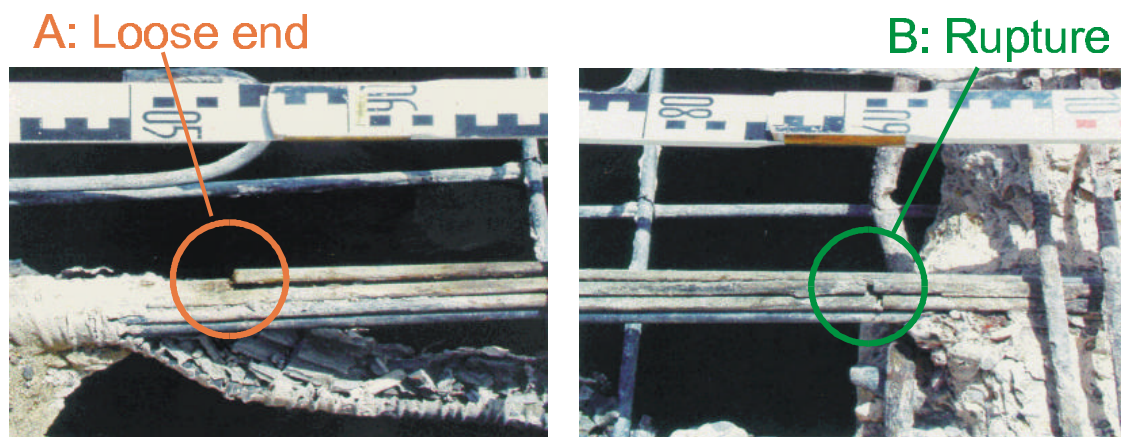


Figure 12. By opening the bridge deck, the indications A and B were confirmed as a loose end and a rupture.

#### 4. Conclusions and outlook

For two selected aircraft NDE tasks, prototype SQUID systems were developed and tested in realistic environments, demonstrating the practical usability of mobile HTS SQUID in conjunction with the eddy current technique. Equipped with orientation-independent cryogenics (position-independent miniature cryostat or Joule-Thomson machine-cooler) the HTS SQUID gradiometers worked successfully under electromagnetically noisy conditions. An automated test stand for SQUID testing of aircraft wheels, with the wheel slowly rotating and a robot with the SQUID enclosure scanning stepwise along the wheel axis, detects deep cracks smaller than today's limit of conventional eddy current devices. The system was successfully tested in the Lufthansa wheel inspection facility at Frankfurt airport. Another

SQUID system has been successfully operated on a professional fuselage scanner. With subsequent signal processing, second layer cracks were detected adjacent to rivets.

The magnetic stray field technique is well suited to detect ruptures in prestressed steel tendons of concrete bridges. A system utilizing HTS SQUID sensors with unsurpassed high field performance and dynamic range was developed. Stray field as well as remanent field scans of rebars after different premagnetization states were taken. Signals of the mild steel reinforcements (stirrups) were suppressed efficiently using a sophisticated signal analysis including best fit estimation of the stirrup signals, comparing residual field measurements after stirrup magnetization inversion, and crack signal correlation analysis. The applicability under field conditions was demonstrated during bridge measurements. Magnetic indications of rebar cracks were verified by opening the bridge deck.

The upcoming challenge is to assist our industrial partners in further developing the prototypes and finally introducing them into the NDE market.

### **Acknowledgments**

The work reviewed in this paper was jointly conducted by Institut für Schicht- und Ionen-technik, Institut für Festkörperforschung and Zentrallabor für Elektronik at Forschungszentrum Jülich, in conjunction with our industrial and research partners Rohmann GmbH, Frankenthal, Daimler-Chrysler Aerospace Airbus GmbH (DASA), Bremen, Lufthansa Technik AG, Frankfurt, ILK Dresden, University of Giessen (Institute for Applied Physics), Forschungs- und Materialprüfanstalt Baden-Württemberg, Stuttgart, Siempelkamp Prüf- und Gutachtergesellschaft mbH, Dresden, and Bundesanstalt für Straßenwesen, Bergisch-Gladbach. Co-workers were M. Banzet, H. Bousack, A.I. Braginski, M.I. Faley, S. Gärtner, W. Glaas, M. Grünekle, R. Hohmann, D. Lomparski, M. Maus, R. Otto, J. Schubert, W. Wolf, N. Wolters, Y. Zhang, and E. Zimmermann at Forschungszentrum, and K. Allweins, W. Becker, A. Binneberg, U. Gampe, C. Heiden, M. Junger, W.-B. Klemmt, M. v.Kreutzbruck, J. Krieger, R. Mattheus, M. Mück, G. Neudert, and G. Sawade at the partner institutions. Support by German BMBF under contracts No. 13N7249/2 and 13N7429/0 is gratefully acknowledged.

This publication is based partly on the presentation made at the European Research Conference (EURESCO) on "Future Perspectives of Superconducting Josephson Devices": Euroconference on Physics and Application of Multi-Junction Superconducting Josephson Devices, Acquafredda di Maratea, Italy, 1-6 July 2000, organised by the European Science Foundation and supported by the European Commission, Research DG, Human Potential Programme, High-Level Scientific Conferences, Contract HPCFCT-1999-00135.

This information is the sole responsibility of the author and does not reflect the ESF or Community's opinion. The ESF and the Community are not responsible for any use that might be made of data appearing in this publication.

### **References**

- [1] W.G. Jenks, S.S.H. Sadeghi, J.P. Wikswo, *SQUIDS for Nondestructive Evaluation*, Journal of Physics D **30**, 293-323 (1997).
- [2] G.B. Donaldson, A. Cochran, D. McA. McKirdy, *The use of SQUIDS for Nondestructive Evaluation*, in: *SQUID Sensors: Fundamentals, fabrication and applications*, NATO ASI series E, Vol. 329, Ed: H. Weinstock, Kluwer, Dordrecht, pp. 599-628 (1996).
- [3] J.P. Wikswo, *The magnetic inverse problem for NDE*, in: *SQUID Sensors: Fundamentals, fabrication and applications*, NATO ASI series E, Vol. 329, Ed: H. Weinstock, Kluwer, Dordrecht, pp. 629-695 (1996).

- [4] Y. Tavrín, H.-J. Krause, W. Wolf, V. Glyantsev, J. Schubert, W. Zander, H. Bousack, *Eddy current technique with high temperature SQUID for nondestructive evaluation of nonmagnetic metallic structures*, *Cryogenics* **36**, 83-86 (1996).
- [5] M. v. Kreutzbruck, M. Mück, U. Baby, C. Heiden, *Detection of deep lying cracks by eddy current SQUID NDE*, in: *Proceedings of the 7th European Conference on Non-Destructive Testing*, Ed: B. Larsen, 7<sup>th</sup> ECNDT, Broendby, Denmark, pp. 46-52 (1998).
- [6] H.-J. Krause, R. Hohmann, H. Soltner, D. Lomparski, M. Grünekle, M. Banzet, J. Schubert, W. Zander, Y. Zhang, W. Wolf, H. Bousack, A. I. Braginski, M. L. Lucía, E. Zimmermann, G. Brandenburg, U. Clemens, H. Rongen, H. Halling, M. I. Faley, U. Poppe, H. Buschmann, G. Spörl, A. Binneberg, M. Junger, *Mobile HTS SQUID System for Eddy Current Testing of Aircraft*, in: *Review of Progress in Quantitative Nondestructive Evaluation*, Vol. 16, Eds: D.O. Thompson, D.E. Chimenti, Plenum, New York, pp. 1053-1060 (1997).
- [7] R. Hohmann, H.-J. Krause, H. Soltner, M.I. Faley, Y. Zhang, D.F. He, C.A. Copetti, H. Bousack, C. Heiden, A.I. Braginski, *HTS SQUID System with J-T-Cryocooler for Eddy Current Nondestructive Evaluation of Aircraft Structures*, *IEEE Trans. on Appl. Supercond.* **7**, 2860-2865 (1997).
- [8] J. Krieger, H.-J. Krause, U. Gampe, G. Sawade, *Magnetic field measurements on bridges and development of a mobile SQUID system*, *Proc. Intl. Conf. on NDE Techniques for Aging Infrastructure & Manufacturing*, Newport Beach, California, USA, pp. 229-239 (1999).
- [9] J.P. Wikswo, Y.P. Ma, N.G. Sepulveda, D.J. Staton, S. Tan, I.M. Thomas, I.M., *Superconducting Magnetometry: A possible technique for aircraft NDE*, in: *Nondestructive Testing of Aging Aircraft*, Eds: M. T. Valley, N.K. Grande, A.S. Kobayashi, SPIE Proc., Vol. 2001, pp. 164-190 (1993).
- [10] Y.P. Ma, J.P. Wikswo, *Imaging subsurface defects using a SQUID magnetometer*, in: *Review of Progress in QNDE*, Vol. 12, Eds: D.O. Thompson, D.E. Chimenti, Plenum Press, New York, pp. 1137-1143 (1993).
- [11] W.N. Podney, *Eddy current evaluation of airframes using refrigerated SQUIDs*, *IEEE Trans. Appl. Supercond.* **5**, 2490-2492 (1995).
- [12] Y. Zhang, H. Soltner, H.-J. Krause, E. Sodtke, W. Zander, J. Schubert, M. Grünekle, D. Lomparski, M. Banzet, H. Bousack, A.I. Braginski, *Planar HTS Gradiometers with Large Baseline*, *IEEE Trans. on Appl. Supercond.* **7**, 2866-2869 (1997).
- [13] M.L. Lucía, R. Hohmann, M.I. Faley, H. Soltner, H.-J. Krause, G. Spörl, A. Binneberg, W. Wolf, H. Bousack, *Operation of HTS SQUIDs with a Portable Cryostat: a SQUID System in Conjunction with Eddy Current Technique for Non-Destructive Testing*, *IEEE Trans. on Appl. Supercond.* **7**, 2878-2881 (1997).
- [14] R. Hohmann, M. Maus, D. Lomparski, M. Grünekle, Y. Zhang, H.-J. Krause, H. Bousack, A.I. Braginski, C. Heiden, *Aircraft wheel testing with machine-cooled HTS gradiometer system*, *IEEE Trans. on Appl. Supercond.* **7**, 3801-3804 (1997).
- [15] R. Hohmann, D. Lomparski, H.-J. Krause, M. v. Kreutzbruck, W. Becker, *Aircraft wheel testing with remote eddy current technique using a SQUID magnetometer*, to be presented at ASC'00, 17.-22.09.2000, Virginia Beach, to be published in: *IEEE Trans. Appl. Supercond.* (2001).
- [16] M. Mück, *Clin. Phys. Physiol. Meas.* **12**, Suppl. B, 51-57 (1991).
- [17] H.-J. Krause, S. Gärtner, N. Wolters, R. Hohmann, W. Wolf, J. Schubert, W. Zander, Y. Zhang, M. v. Kreutzbruck, M. Mück, *Multiplexed SQUID Array for Non-Destructive Evaluation of Aircraft Structures*, to be presented at ASC'00, 17.-22.09.2000, Virginia Beach, to be published in: *IEEE Trans. Appl. Supercond.* (2001).
- [18] G. Sawade J. Straub, H.-J. Krause, H. Bousack, G. Neudert, R. Ehrlich, *Signal analysis methods for remote magnetic examination of prestressed elements*, *Proc. Intl. Sympos. on NDT in Civil Engineering (NDT-CE)*, Vol.II, DGZfP, Berlin, pp.1077-1084 (1995).
- [19] H. Scheel, *Spannstahlbruchortung an Spannbetonbauteilen mit nachträglichem Verbund unter Ausnutzung des Remanenzmagnetismus*, Ph.D. Thesis, D 83, Technical University Berlin, Berlin (1997).
- [20] G. Sawade, U. Gampe, H.-J. Krause, *Non Destructive Examination of Prestressed Tendons by the Magnetic Stray Field Method*, in: *Proc. 4<sup>th</sup> Conf. on Engineering Structural Integrity Assessment*, Cambridge, U.K., pp. 353-363 (1998).

- [21] A. Ghorbanpoor, *Magnetic-based NDE of steel in prestressed and post-tensioned concrete bridges*, Proc. Structural Materials Technology III, San Antonio, Texas, pp. 343-349 (1998).
- [22] M.I. Faley, U. Poppe, K. Urban, E. Zimmermann, W. Glaas, H. Halling, M. Bick, H.-J. Krause, D.N. Paulson, T. Starr, and R.L. Fagaly, *Operation of the HTS dc-SQUID Sensors in High Magnetic Fields*, IEEE Trans. Appl. Supercond. **9**, 3386-3391 (1999).
- [23] E. Zimmermann, G. Brandenburg, U. Clemens, H. Rongen, H. Halling, H.-J. Krause, R. Hohmann, H. Soltner, D. Lomparski, M. Grünekle, K.-D. Husemann, H. Bousack, A.I. Braginski, *HTS-SQUID Magnetometer with Digital Feedback Control for NDE Applications*, in: *Review of Progress in Quantitative Nondestructive Evaluation*, Vol. 16B, Eds: D.O. Thompson, D.E. Chimenti, Plenum, New York, pp. 2129-2135 (1997).
- [24] J. Krieger, E. Rath, H.-J. Krause, *Anwendung zerstörungsfreier Prüfverfahren bei Betonbrücken: Messungen an der Talbrücke Michelsrombach*, Berichte der BAST, Bergisch Gladbach, in press (2000).
- [25] H.-J. Krause, W. Wolf, W. Glaas, E. Zimmermann, M.I. Faley, G. Sawade, G. Neudert, U. Gampe, J. Krieger, *SQUID system for magnetic inspection of prestressed tendons on concrete bridges*, to be published in: Proceedings of the 15<sup>th</sup> World Conference on Non-destructive Testing, Rom, 15.-21.10.2000.